Experimental Identification of Spin-Parities and Single-Particle Configurations in ^{257}No and Its α-Decay Daughter ^{253}Fm

M. Asai,[1] K. Tsukada,[1] M. Sakama,[2] S. Ichikawa,[1] T. Ishii,[3] Y. Nagame,[1] I. Nishinaka,[1] K. Akiyama,[1] A. Osa,[3] Y. Oura,[4] K. Sueki,[5] and M. Shibata[6]

[1]*Advanced Science Research Center, Japan Atomic Energy Research Institute, Tokai, Ibaraki 319-1195, Japan*
[2]*Department of Radiologic Science and Engineering, The University of Tokushima, Tokushima 770-8509, Japan*
[3]*Department of Materials Science, Japan Atomic Energy Research Institute, Tokai, Ibaraki 319-1195, Japan*
[4]*Department of Chemistry, Tokyo Metropolitan University, Hachioji, Tokyo 192-0397, Japan*
[5]*Department of Chemistry, University of Tsukuba, Tsukuba, Ibaraki 305-8571, Japan*
[6]*Radioisotope Research Center, Nagoya University, Nagoya 464-8602, Japan*

(Received 6 April 2005; published 2 September 2005)

α-γ and α-electron coincidence spectroscopy for a short-lived heavy actinide nucleus ^{257}No ($T_{1/2} =$ 24.5 s) has been performed using a gas-jet transport system and an on-line isotope separator. Spin-parities of excited states in ^{253}Fm fed by the α decay of ^{257}No have been identified on the basis of the measured internal conversion coefficients. The $\nu 3/2^+[622]$ configuration has been assigned to the ground state of ^{257}No as well as to the 124.1 keV level in ^{253}Fm. It was found that the ground-state configuration of ^{257}No is different from that of lighter $N = 155$ isotones.

DOI: 10.1103/PhysRevLett.95.102502 PACS numbers: 21.10.Hw, 23.20.Lv, 23.20.Nx, 27.90.+b

The stability of superheavy nuclei caused by nuclear shell effects is one of the most interesting subjects in nuclear physics. So far, many theoretical studies have predicted shell structure of superheavy nuclei, while the experimental information is very scarce. In particular, little is known about spin-parities, single-particle configurations of ground states as well as excited states, and excitation energies of the levels. The shell structure strongly depends on the single-particle energies. The experimental identification of single-particle states in odd-mass superheavy nuclei allows us to extract energy spacings and order of the single-particle states that provide sensitive and direct information on the shell structure of superheavy nuclei.

Experimentally, the deformed neutron shell gap at $N = 152$ has been found from systematics of mass and half-life values, and Nilsson single-particle energies in $Z \leq 100$ nuclei. Recently, in-beam γ-ray spectroscopy coupled with a recoil-decay tagging technique was used to successfully study excited states in ^{250}Fm, ^{251}Md, and $^{252-254}$No [1], and γ rays following the α decay of ^{253}No ($T_{1/2} =$ 1.7 min) and ^{255}Rf (1.6 s) were measured using the velocity filter SHIP at GSI [2,3]. These studies provided experimental information on excited states in $Z \geq 100$ and $N \leq 152$ nuclei. On the other hand, the next deformed neutron shell gap was suggested at $N = 162$ [4–6]. However, the neutron single-particle states in $N > 152$ nuclei have never been established through γ-ray spectroscopy except for the ground states of long-lived nuclei ^{253,255,257}Fm$_{153,155,157}$ [7–9] and their daughters. The aim of the present study is to establish Nilsson single-particle states in odd-mass $Z > 100$ and $N > 152$ nuclei through experimental spin-parity assignments for ground states as well as excited states by means of α-γ and α-e (internal conversion electron) coincidence spectroscopy. In this Letter, we report our first result on the α decay of ^{257}No$_{155}$, which is one of the heaviest nuclei whose spin-parity is assigned experimentally.

The nucleus ^{257}No was produced by the ^{248}Cm(^{13}C, $4n$) reaction using the JAERI tandem accelerator. Two kinds of experiments were carried out; one was an α-γ coincidence measurement using a rotating wheel system coupled with a gas-jet transport system, and the other was an α-e coincidence measurement using a gas-jet coupled on-line isotope separator (ISOL). In the α-γ experiment, a ^{248}Cm target (96.7% ^{248}Cm, 0.04% ^{247}Cm, 3.1% ^{246}Cm, 0.15% ^{245}Cm, 0.008% ^{244}Cm) electrodeposited on a 2.1 mg/cm^2 beryllium backing foil was bombarded with a ^{13}C beam with an average intensity of 230 particle-nA. The beam energy was 70 MeV on target, and the effective target thickness was about 300 μg/cm^2. Reaction products recoiling out of the target were thermalized in He gas loaded with KCl clusters, transported through a 25 m long capillary with a He jet [10], and finally deposited on a polyethylene terephthalate foil with a 20 mm diameter and 120 μg/cm^2 thickness, forty of which were set on the periphery of a rotating wheel. The wheel periodically rotated by 63° at 60 s intervals, and moved the deposited sources to two consecutive detector stations. At the detector stations, the foil was sandwiched between two Si PIN photodiode detectors (Hamamatsu S3204-09, 18×18 mm^2 active area) to detect α particles with 78% efficiency, and two Ge detectors (ORTEC LOAX and GMX) were placed just behind the two Si detectors. The efficiency of each Ge detector was determined to be ~15% for 60–120 keV γ rays and ~4% at 25 keV using a mixed γ-ray standard source. The energy calibration curves were measured using the same source before and after the on-line experiment. α singles and α-γ

coincidence events were recorded during 36 h in an event-by-event mode together with time information.

For the α-e coincidence experiment, two ^{248}Cm targets with thicknesses of 240 and 300 $\mu g/cm^2$ were placed in the target chamber with 15 mm between them, and bombarded with a ^{13}C beam with an average intensity of 370 particle-nA. The beam energies were 76 MeV on the first target and 69 MeV on the second one. Reaction products were transported by a He/PbI$_2$ aerosol jet into a surface ionization-type thermal ion source of the ISOL [11]. Ionized products were accelerated with 30 kV and were mass-separated with a resolution of $M/\Delta M \sim 800$. The overall efficiency of this gas-jet coupled ISOL system was measured to be 0.46% for ^{257}No. The separated ions were continuously implanted into a Si PIN photodiode (Hamamatsu S3590-09, 9×9 mm^2, 0.3 mm^t) which was tilted 45° with respect to the ion beam axis (this detector is called "Si-1"). Another three photodiodes (called "Si-2, 3, and 4") were placed around Si-1 to detect α particles and electrons [12] simultaneously. The detection efficiencies for α particles from the implanted nuclei were 50%, 20%, 4.7%, and 4.6% for Si-1, 2, 3, and 4, respectively. The detectors were cooled at $-10\,^\circ$C to reduce dark current. The energy calibration of the Si detectors was carried out before and after the on-line experiment using an ^{241}Am α source and mass-separated ^{221}Fr implanted into Si-1 by the present ISOL system. The α energy was calibrated using the α lines of ^{221}Fr and its α-decay daughters ^{217}At and ^{213}Po. The electron energy was calibrated using the K and L internal conversion electron (ICE) lines associated with the 218.2 keV γ transition observed in coincidence with the 6126 keV α particles of ^{221}Fr, and the L ICE line of the 59.5 keV γ transition in ^{241}Am. The energy resolution of the detectors (full width at half maximum) was 2.8 keV for 38 keV electrons, 2.1 keV for 59.5 keV γ rays, and 25–30 keV for 6341 keV α particles. α singles, electron singles, and all the combinations of coincidence events were recorded event by event during 115 h.

Figure 1 shows an α singles spectrum obtained in the α-γ experiment. A total of 5200 α particles from the decay of ^{257}No were observed. The half-life of 24.5(5) s was derived from its decay curve as shown in the inset of Fig. 1. This half-life agrees well with a reported value of 26(2) s [13]. Figures 2(a)–2(c) show α singles spectra for the mass-separated ^{257}No source measured by Si-1, 2, and 3, respectively. Since the detection efficiency of Si-1 is 50%, the coincidence summing effect between α particles and ICEs strongly distorts the Si-1 spectrum. The α component around 8270 keV in the Si-1 spectrum was attributed to the coincidence summing peak because it disappears in the Si-3 spectrum. The relative intensity of the 8323 keV α peak in the Si-1 spectrum is also larger than those in the Si-2 and 3 spectra, but it does not disappear in the Si-3 spectrum. Thus, we concluded that it is a true α transition. The α energies and intensities were determined using the Si-2, 3, and 4 spectra as 8222(6) keV with an intensity of 83(2)% and 8323(7) keV with 17(2)%.

A γ-ray spectrum in coincidence with α particles of ^{257}No is shown in Fig. 3(a). Three γ transitions of 77.0, 101.8, and 124.1 keV and Fm L x rays were clearly observed. These γ rays were coincident with the 8222 keV α particles as shown in Fig. 4(a). In addition, the 136.4 keV γ events were weakly observed in coincidence with 8167–8195 keV α particles. The emission probability of the 77.0 keV γ ray was determined to be 2.0(4) per 100 α decays.

Figure 3(b) shows a sum of electron spectra detected by Si-2, 3, and 4 in coincidence with the 7500–8500 keV α particles. Two prominent electron peaks were observed at 50.0(8) and 97.4(8) keV, which correspond to the L ICEs of the 77.0 and 124.1 keV γ transitions in ^{253}Fm, respectively. The M electron peaks were observed as well. The L and M electron peaks of the 101.8 keV transition are not clearly seen, probably due to low statistics. As shown in Fig. 4(b), the 8323 keV α particles were coincident only with low-energy electrons of <25 keV, while the >25 keV electrons were coincident with the 8222 keV α transition.

From the measured electron to γ intensity ratios, $L_1 + L_2$ internal conversion coefficients ($\alpha_{L_1+L_2}$) of the 77.0,

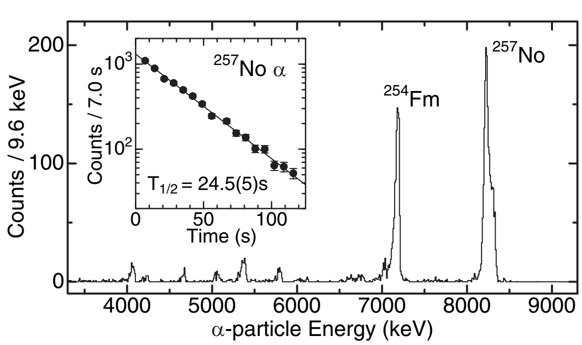

FIG. 1. α-singles spectrum obtained in the α-γ experiment. The inset shows a decay curve of α particles of ^{257}No. The nucleus ^{254}Fm is also produced in the ^{248}Cm + ^{13}C reaction system.

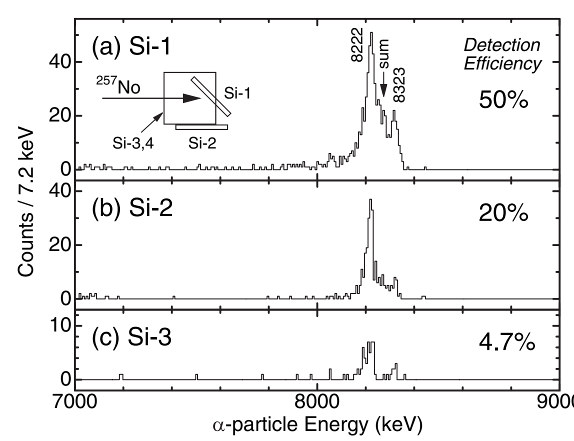

FIG. 2. α-singles spectra measured in the α-e experiment with (a) Si-1, (b) Si-2, and (c) Si-3 whose detection efficiencies are 50%, 20%, and 4.7%, respectively. The detector configuration is depicted in the figure.

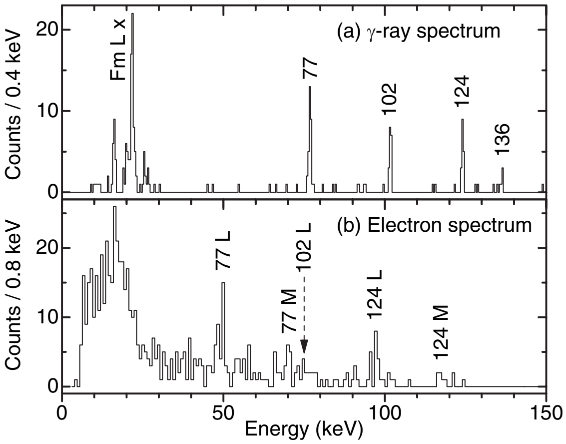

FIG. 3. (a) γ-ray spectrum in coincidence with α particles of ^{257}No. (b) A sum of electron spectra detected by Si-2, 3, and 4 in coincidence with α particles of ^{257}No.

101.8, 124.1, and 136.4 keV transitions were deduced to be 10(3), <8.3, 5.4(26), and <3.8, respectively. From the comparison between the experimental and theoretical $\alpha_{L_1+L_2}$ [14] shown in Fig. 5(a), the $M1$ multipolarity is assigned to the 77.0 keV transition. The multipolarity of the 124.1 keV transition whose $\alpha_{L_1+L_2}$ is consistent with both $M1$ and $E2$ is determined through the measured L_3 electron intensity. Figure 5(b) shows theoretical electron spectra of the 124.1 keV $E2$ and $M1$ transitions [14] compared with the measured one. The intensity of the L_3 electrons of the $E2$ transition is about a half of that of the $L_1 + L_2$ electrons, while that of the $M1$ transition is negligibly small. The observed electron spectrum does not show such a large L_3 electron component. Although a small number of counts are seen at ~102 keV, its energy is lower than that of the L_3 electron; this component would arise from the coincidence summing effect between L_1 electrons and the following low-energy x rays or Auger electrons. Even if this component were L_3 electrons, the deduced $E2/M1$ mixing could reach only 43 ± 10%. Therefore, it is concluded that the 124.1 keV transition is $M1$ dominant, not a pure $E2$ transition.

On the basis of the α- and γ-transition energies, α-γ, α-e, and e-e coincidence relationships, the decay scheme of ^{257}No has been established as shown in Fig. 6. The 136.4 keV γ transition is incorporated between the 158.7

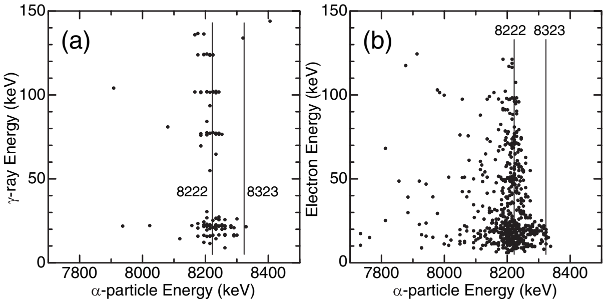

FIG. 4. (a) α-γ and (b) α-e coincidence matrices.

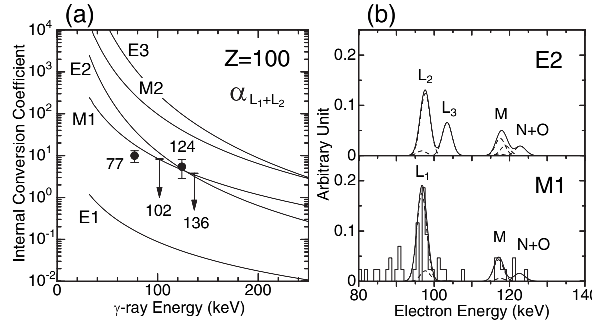

FIG. 5. (a) $L_1 + L_2$ internal conversion coefficients ($\alpha_{L_1+L_2}$) of the 77.0, 101.8, 124.1, and 136.4 keV transitions compared with the theoretical $\alpha_{L_1+L_2}$ of $Z = 100$ nuclei [14]. (b) Theoretical electron spectra of the 124.1 keV $E2$ and $M1$ transitions in $Z = 100$ nuclei [14]. Solid lines represent the sum of $L_1 - L_3$, $M_1 - M_5$, N, and O ICE components. Each of the components is represented by dashed lines. The measured electron spectrum is also depicted in the bottom panel by histograms.

and 22.3 keV levels by taking into account the coincident α energies. The α-transition intensity to the 158.7 keV level is estimated to be <4% from the intensities of γ rays and total internal conversion coefficients. Although the 22.3, 24.8, and 47.1 keV γ rays were not observed because of their large internal conversion coefficients, low-energy electrons associated with these transitions were observed in coincidence with the 8323 keV α particles and with the 50 keV electrons in the e-e coincidence data.

The spin-parity of the ground state of ^{253}Fm is known to be $1/2^+$ with the $1/2^+[620]$ configuration [7]. Since the 124.1 keV transition is predominantly $M1$, the spin-parity of the 124.1 keV level is restricted to either $1/2^+$ or $3/2^+$. The 124.1 keV level is populated by the favored α transition with a hindrance factor of 1.3, indicating that the 124.1 keV level is a Nilsson single-particle state whose orbital is the same as that of the ground state of ^{257}No. Among the Nilsson single-particle states with $\Omega = 1/2^+$ or $3/2^+$, only the $3/2^+[622]$ state could lie at such low energy in ^{253}Fm except the $1/2^+[620]$ ground state. Thus, we have assigned the $3/2^+[622]$ configuration to the 124.1 keV level in ^{253}Fm as well as to the ground state of

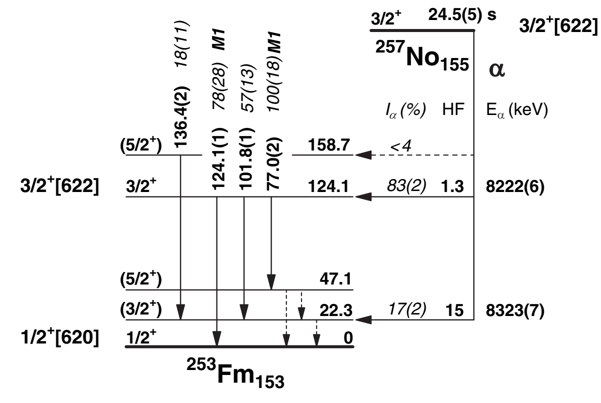

FIG. 6. Proposed decay scheme of ^{257}No.

^{257}No. The 22.3 and 47.1 keV levels are considered to be the $3/2^+$ and $5/2^+$ states in the $1/2^+[620]$ band, respectively, because their energies are very close to those of the $1/2^+[620]$ band in neighboring nuclei. Note that the hindrance factor of 15 for the 8323 keV α transition seems small for the transition between the different configurations. It may suggest that a configuration mixing would occur in the $3/2^+$ states, though further detailed studies are needed to clarify it. The energy spacing between the 124.1 and 158.7 keV levels is in good agreement with that between the $3/2^+$ and $5/2^+$ states in the $3/2^+[622]$ band in ^{249}Cm and ^{251}Cf, both of which are 34 keV.

The ground-state configuration of $3/2^+[622]$ for ^{257}No assigned in the present work is different from that of $7/2^+[613]$ for the lighter $N = 155$ isotones, ^{253}Cf and ^{255}Fm. This explains why the α-decay pattern is different for ^{257}No (as noted in Refs. [13,15]) than for the lighter isotones ^{253}Cf and ^{255}Fm in which more than 98% of the α decay proceeds via the $7/2^+[613] \rightarrow 7/2^+[613]$ transition, while in ^{257}No two different α groups are observed. In the $N = 153$ isotones, excitation energy of the $3/2^+[622]$ state decreases with increasing proton number as 208, 178, and 124 keV in ^{249}Cm, ^{251}Cf, and ^{253}Fm, respectively, while that of the $7/2^+[613]$ state increases as 49 and 106 keV in ^{249}Cm and ^{251}Cf, respectively. This trend can be explained by the crossing between the downsloping $3/2^+[622]$ and upsloping $7/2^+[613]$ orbitals on the Nilsson diagram. The change of the ground-state configuration between ^{257}No and the lighter $N = 155$ isotones would also result from the gradually increasing quadrupole deformation with increasing proton number.

There are some theoretical calculations for Nilsson single-particle energies around ^{257}No [16–19]. Ćwiok *et al.* [16] predicted the $1/2^+[620]$ ground state for ^{257}No and the nearly degenerate $3/2^+[622]$ state at 0.01 MeV using the Nilsson-Strutinsky approach with an average Woods-Saxon potential. Although they could not reproduce the $7/2^+[613]$ ground state for ^{253}Cf and ^{255}Fm, their calculation successfully showed that the energy of the $7/2^+[613]$ state relative to the $3/2^+[622]$ one increases with the proton number in both $N = 153$ and 155 isotones. On the other hand, a recent Hartree-Fock-Bogoliubov calculation with a Skyrme interaction succeeded in predicting the $3/2^+[622]$ ground state for ^{257}No [18], though they did not show the calculation for lighter neighboring nuclei.

In conclusion, excited states in ^{253}Fm populated via the α decay of ^{257}No have been established through α-γ and α-e coincidence spectroscopy. Spin-parities of the excited states in ^{253}Fm as well as the ground state of ^{257}No have been identified. The $3/2^+[622]$ configuration has been assigned to the ground state of ^{257}No, which is different from the ground state of other $N = 155$ isotones ^{253}Cf and ^{255}Fm with the $7/2^+[613]$ configuration. The present results demonstrated that experimental spin-parity assignments are essential to clarify the shell structure of superheavy nuclei. α-γ and α-e coincidence spectroscopy is one of the best methods to extend the experimental studies to heavier nuclei.

We thank the crew of the JAERI tandem accelerator for generating an intense and stable ^{13}C beam. This work was supported by a Grant-in-Aid for Scientific Research of Ministry of Education, Culture, Sports, Science and Technology of Japan.

[1] R.-D. Herzberg, J. Phys. G **30**, R123 (2004), and references therein.
[2] F. P. Heßberger, S. Hofmann, D. Ackermann, V. Ninov, M. Leino, G. Münzenberg, S. Saro, A. Lavrentev, A. G. Popeko, A. V. Yeremin, and Ch. Stodel, Eur. Phys. J. A **12**, 57 (2001).
[3] F. P. Heßberger, S. Hofmann, D. Ackermann, P. Cagarda, R.-D. Herzberg, I. Kojouharov, P. Kuusiniemi, M. Leino, and R. Mann, Eur. Phys. J. A **22**, 417 (2004).
[4] S. Hofmann, F. P. Heßberger, D. Ackermann, G. Münzenberg, S. Antalic, P. Cagarda, B. Kindler, J. Kojouharova, M. Leino, B. Lommel, R. Mann, A. G. Popeko, S. Reshitko, S. Śaro, J. Uusitalo, and A. V. Yeremin, Eur. Phys. J. A **14**, 147 (2002).
[5] P. Möller and J. R. Nix, J. Phys. G **20**, 1681 (1994).
[6] R. Smolańczuk, J. Skalski, and A. Sobiczewski, Phys. Rev. C **52**, 1871 (1995).
[7] I. Ahmad, A. M. Friedman, R. F. Barnes, R. K. Sjoblom, J. Milsted, and P. R. Fields, Phys. Rev. **164**, 1537 (1967).
[8] F. Asaro, S. Bjørnholm, and I. Perlman, Phys. Rev. **133**, B291 (1964).
[9] F. Asaro and I. Perlman, Phys. Rev. **158**, 1073 (1967).
[10] Y. Nagame, M. Asai, H. Haba, S. Goto, K. Tsukada, I. Nishinaka, K. Nishio, S. Ichikawa, A. Toyoshima, K. Akiyama, H. Nakahara, M. Sakama, M. Schädel, J. V. Kratz, H. W. Gäggeler, and A. Türler, J. Nucl. Radiochem. Sci. **3**, 85 (2002).
[11] S. Ichikawa, K. Tsukada, M. Asai, H. Haba, M. Sakama, Y. Kojima, M. Shibata, Y. Nagame, Y. Oura, and K. Kawade, Nucl. Instrum. Methods Phys. Res., Sect. B **187**, 548 (2002).
[12] I. Ahmad, R. R. Betts, T. Happ, D. J. Henderson, F. L. H. Wolfs, and A. H. Wuosmaa, Nucl. Instrum. Methods Phys. Res., Sect. A **299**, 201 (1990).
[13] P. Eskola, K. Eskola, M. Nurmia, and A. Ghiorso, Phys. Rev. C **2**, 1058 (1970).
[14] F. Rösel, H. M. Fries, K. Alder, and H. C. Pauli, At. Data Nucl. Data Tables **21**, 91 (1978).
[15] C. M. Gannett, R. B. Chadwick, K. B. Chen, K. R. Czerwinski, K. E. Gregorich, H. L. Hall, R. A. Henderson, D. M. Lee, J. D. Leyba, M. J. Nurmia, and D. C. Hoffman, LBL-27840, 1988, p. 45.
[16] S. Ćwiok, S. Hofmann, and W. Nazarewicz, Nucl. Phys. **A573**, 356 (1994).
[17] P. Möller, J. R. Nix, and K.-L. Kratz, At. Data Nucl. Data Tables **66**, 131 (1997).
[18] W. Nazarewicz, M. Bender, S. Ćwiok, P. H. Heenen, A. T. Kruppa, P.-G. Reinhard, and T. Vertse, Nucl. Phys. **A701**, 165c (2002).
[19] J. F. Berger, D. Hirata, and M. Girod, Acta Phys. Pol. B **34**, 1909 (2003).